Received 20 December 2016; revised 15 January 2017; accepted 19 January 2017. Date of publication 23 January 2017; date of current version 22 February 2017. The review of this paper was arranged by Editor C. C. McAndrew.

Digital Object Identifier 10.1109/JEDS.2017.2656883

A Model for Neutral Defect Limited Electron Mobility in Strained-Silicon Inversion Layers

SHANG-HSUN HSIEH AND MING-JER CHEN (Senior Member, IEEE)

Institute of Electronics, National Chiao Tung University, Hsinchu 300, Taiwan

CORRESPONDING AUTHOR: M.-J. CHEN (e-mail: chenmj@faculty.nctu.edu.tw)

This work was supported by the Ministry of Science and Technology of Taiwan under Contract MOST 104-2221-E-009-072-MY3.

ABSTRACT On the strained silicon metal–oxide–semiconductor field-effect transistors (MOSFETs), we show how to derive a formalism dealing with the scattering of a 2-D electron by a neutral defect. The corresponding neutral defect limited inversion-layer electron mobility, μ_n, is calculated in the momentum relaxation time approximation. The calculated results lead to a new analytical model: $\mu_n = cN_n^{-1}$, where N_n is the neutral defect density per unit area and c is the coefficient independent of the inversion-layer density, the strain, and the temperature. The validity and applicability of the model are confirmed by citing three independent experiments on strained silicon MOSFETs undergoing different implantation sources and different annealing budgets. Importantly, this paper clarifies for the first time that strain will not change neutral defect limited mobility unless changing the neutral defect density. This reasonably explains the two experimental observations during implantation and annealing: 1) the implantation-induced strain relaxation in strained sample does not occur and 2) the neutral defect density is much higher in strained sample than in unstrained sample.

INDEX TERMS Interstitial, metal-oxide-semiconductor field-effect transistors (MOSFETs), mobility, neutral defect, scattering, strain.

I. INTRODUCTION

Owing to the incomplete ionization in doped semiconductors at low temperatures, the donors or acceptors can be classified into two different impurities: One of ionized impurity and one of neutral impurity. Neutral impurity scattering of 3D electrons has been well theoretically studied using both a hydrogen-like scattering center [1] and a square-well potential based scattering center [2]. The partial-wave technique (see [1]–[4] and the references therein) was adopted to calculate the scattering cross-section. For the scattering by a hydrogen-like impurity, Erginsoy [1] put forward the creation of an analytical expression for the zero-order phase shift δ_0 associated with partial waves, which yielded $\sin \delta_0 \approx 0.9$. By solving the Schrödinger equations within and outside of the potential well (see Fig. 1), Sclar [2] derived the following analytical formula:

$$\sin \delta_0 = \frac{\sqrt{E_k}}{\sqrt{E_k + E_T}} \quad (1)$$

where E_K is the electron kinetic energy and E_T is the binding energy ($\approx$ 2 meV for silicon [2], [3]). Corresponding neutral impurity limited 3D electron mobility expressions have been devised [1]–[4]. Note that in the derivation process [2], [3], both the potential depth V_0 and potential width r_T were initially accounted for, but under some criteria subsequently satisfied, both of them disappear in the formation of (1).

On the other hand, for doped semiconductors at room temperature, there are process-induced interstitials in terms of the impurity and/or host atoms that are dislocated from the lattice sites. Such lattice defects are electrically neutral and can behave like neutral impurities. Indeed, Eq. (1) can provide a good understanding of neutral defect scattering. For $E_T \gg E_k$, the scattering cross-section (proportional to the square of $\sin\delta_0$) goes to zero and thereby the defect cannot scatter any electrons. But for $E_T << E_k$, the cross section ($\sin\delta_0 \approx 1$) is significantly large and hence the scattering is very strong, constituting the so-called neutral defect scattering.

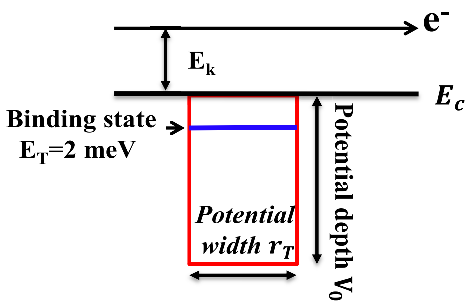

FIGURE 1. Schematics of a square-well potential as the scattering center of a neutral defect [3]. E_T is the binding energy below the conduction-band edge and is equal to 2 meV for silicon [2], [3]. The depth of the potential V_0 is assumed to be much larger than E_T in the derivation of Eq. (1) [3]. The width of the potential r_T is the size of the interstitial (~2 Å) [3]. E_K is the kinetic energy of conduction-band electrons.

Recently, the significance of the neutral defects in short-channel MOSFETs was experimentally demonstrated [5]. The underlying inversion-layer electron mobility component due to neutral defects alone was also experimentally extracted [5]. To extract the neutral defect density underlying the short-channel inversion-layer mobility degradation [5], we proposed a 2D scattering formalism in our previous work [6]. However, the derivation of the formalism [6] was not fully detailed; even the impact of the strain was not clarified in use of the formalism [6]. Checking the applicability of the formalism in the area of strain engineering is crucial.

In this paper, we present a comprehensive, detailed derivation procedure toward the creation of the 2D scattering formalism, taking into account the impact of strain. We prove for the first time that Eq. (1) can hold for a 2D electron gas. Then a sophisticated inversion-layer electron mobility calculation task is performed, for different combinations of the defect density, the inversion-layer density, the uniaxial and biaxial tensile stress, and the temperature. A new analytical model of neutral defect limited electron inversion-layer mobility is drawn, followed by the experimental validation of the model.

II. FORMALISM DERIVATION

Methods for treating quantum confinement and quantum scattering in strained-silicon inversion layers existed [7]–[11]. For a subband of 2D electron gas (2DEG), its scattering cross-section by neutral defects can be written as

$$\sigma = \frac{2}{\pi}\int_0^{2\pi} d\theta \frac{\sin^2\delta_0}{k} \tag{2}$$

where θ is the scattering angle and k is the electron wave vector. As will be explained later in the Appendix, Eq. (1) is valid in the case of 2DEG. Thus, by substituting (1) for $\sin\delta_0$ in (2), we obtain

$$\sigma = \frac{4}{k}\frac{E_k}{E_k + E_T} \tag{3}$$

Obviously, for $E_T \rightarrow 0$ or $E_T << E_k$, the cross-section around the defect can have a large value making it a strong scattering center. In (3), E_k is equal to the electron energy E minus the subband level energy $E_{subband}$. The corresponding relaxation (or collision) time due to neutral defects reads as

$$\frac{1}{\tau_n(E)} = N_n \upsilon \sigma \tag{4}$$

where N_n is the neutral defect density per unit area and υ is the electron velocity. Using $\upsilon = \hbar k/m^*$ for a parabolic subband in the transport direction, Eq. (4) becomes

$$\frac{1}{\tau_n(E)} = \frac{4\hbar N_n}{m^*}\frac{E - E_{subband}}{E - E_{subband} + E_T} \tag{5}$$

Eq. (5) can be rewritten in general form:

$$\frac{1}{\tau_n^{ij}(E)} = \frac{4\hbar N_n}{m_j^*}\frac{E - E_{ij}}{E - E_{ij} + E_T} \tag{6}$$

Taking silicon as example, $j = 1$ in (6) represents the twofold valley $\Delta 2$, $j = 2$ the fourfold valley $\Delta 4$, and i the corresponding subband number. The neutral defect limited mobility component of subband i of valley j can be calculated in the momentum relaxation time approximation:

$$\mu_n^{ij} = \frac{q\int_{E_{ij}}^{\infty}\left(E - E_{ij}\right)\tau_n^{ij}(E)\left(\frac{\partial f}{\partial E}\right)dE}{m_j^*\int_{E_{ij}}^{\infty}\left(E - E_{ij}\right)\left(\frac{\partial f}{\partial E}\right)dE} \tag{7}$$

where f is the Fermi-Dirac distribution. It can be easily seen that through a combination of (6) and (7), the resulting μ_n^{ij} does not contain the effective mass m_j^*. By going through all valleys and subbands, neutral defect limited 2D electron mobility can be obtained as follows:

$$\mu_n = \sum_{ij}\mu_n^{ij}p^{ij} \tag{8}$$

where p^{ij} is the fractional population of subband i of valley j.

Note that in the presence of the non-parabolicity α in bands, above m_j^* should be replaced by $m_j^*(1 + 2\alpha E)$. Fortunately, the resulting component μ_n^{ij} does not contain the term $m_j^*(1 + 2\alpha E)$. In the quasi-equilibrium case, the parabolic band is a good approximation and thereby the population p^{ij} is not affected by the parabolicity. Thus, use of the parabolic band is validated in the derivation of the μ_n formalism.

III. SIMULATION AND MODEL

We have previously established a sophisticated simulation package [12]–[14] consisting of a self-consistent Poisson and Schrödinger's equations solver with the existing strain Hamiltonian [11] incorporated and an experimentally calibrated inversion-layer electron mobility calculation program. Eq. (6) has been added to the latter program, through the momentum relaxation time approximation.

For given neutral defect density, the simulated neutral defect limited electron inversion-layer mobility μ_n at 300 K is found to be independent of the strain, as shown in

Fig. 2 for uniaxial tensile stress and in Fig. 3 for biaxial tensile stress. The calculated μ_n is considerably constant over three decades of inversion-layer densities. The calculated temperature dependence is weak, too (not shown here but can be found elsewhere [6]). Also plotted in Fig. 2 and 3 are calculated total mobility curves for uniaxial stress and biaxial stress, respectively, due to the combination of ionized impurity scattering, phonon scattering, surface roughness scattering, and neutral defect scattering. Both figures show expected mobility enhancement for the conventional scatterers, not the neutral defect scattering alone. We also found from the self-consistent Poisson and Schrödinger's equations solver that the Fermi level minus the lowest subband level increases with tensile strain.

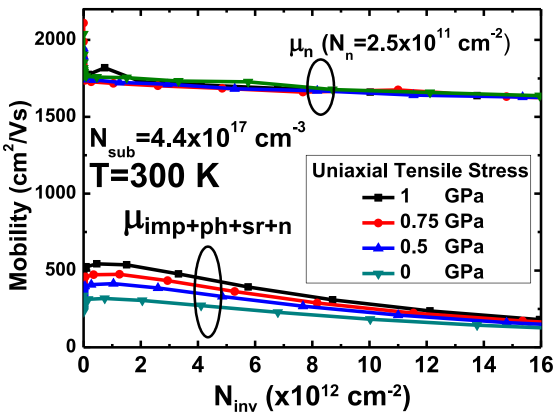

FIGURE 2. Calculated neutral defect limited electron inversion-layer mobility and total mobility due to the combination of ionized impurity scattering, phonon scattering, surface roughness scattering, and neutral defect scattering versus inversion-layer density for different uniaxial tensile stresses.

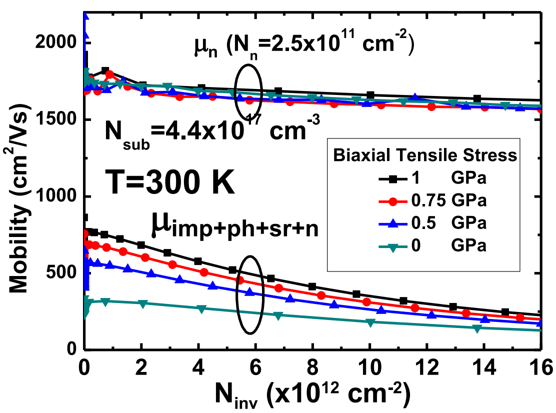

FIGURE 3. Calculated neutral defect limited electron mobility and total mobility due to the combination of ionized impurity scattering, phonon scattering, surface roughness scattering, and neutral defect scattering versus inversion-layer density with biaxial tensile stress as a parameter.

The calculated neutral defect limited electron mobility μ_n for different N_{inv} is shown in Fig. 4 versus defect density N_n. Obviously, μ_n is proportional to the reciprocal of N_n while being independent of N_{inv} as mentioned above. Therefore, we can empirically write an analytical model: $\mu_n = cN_n^{-1}$ where c is constant.

Experimentally speaking, use of Matthiessen's rule is inevitable to extract neutral defect limited mobility or neutral defect density, as detailed in [5] and [15]. In this sense, we do extra simulation in the framework of Matthiessen's rule. Results with and without neutral defect scattering are shown in Fig. 5 for uniaxial tensile stress and

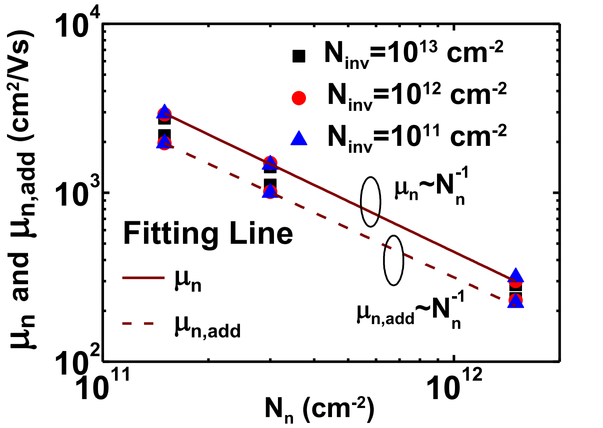

FIGURE 4. The calculated neutral defect limited mobility μ_n from (8) and $\mu_{n,add}$ from (9), plotted versus neutral defect density with inversion layer density as a parameter. Also plotted are fitting lines.

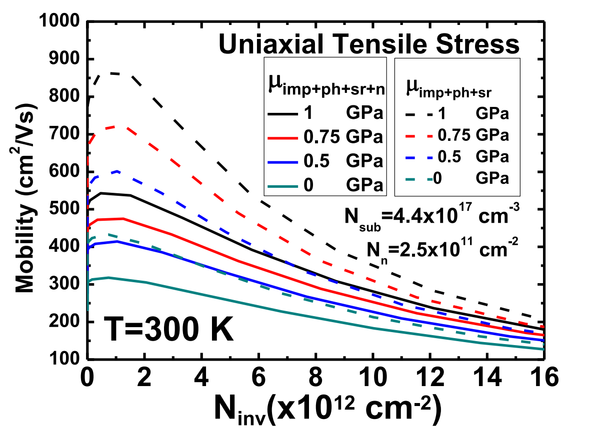

FIGURE 5. Calculated electron mobility due to ionized impurity scattering, phonon scattering, and surface roughness scattering, with (solid lines) and without (dashed lines) neutral defect scattering, versus inversion-layer density for different uniaxial tensile stresses.

Fig. 6 for biaxial tensile stress. Consequently, according to Matthiessen's rule the expression for neutral defect limited electron mobility $\mu_{n,add}$ can be obtained:

$$\mu_{n,add}^{-1} = \mu_{imp+ph+sr+n}^{-1} - \mu_{imp+ph+sr}^{-1} \tag{9}$$

where $\mu_{imp+ph+sr}$ represents the conventional total inversion-layer effective mobility due to the combination of ionized impurity scattering, phonon scattering and surface roughness scattering. Resulting $\mu_{n,add}$ values are the same between with and without uniaxial or biaxial stress, as added to Fig. 4.

They apparently stay below μ_n with the same slope of the fitting line, leading to

$$\mu_{n,add} = 1000 \times \frac{3 \times 10^{11}\, cm^{-2}}{N_n} cm^2/Vs \qquad (10)$$

Again, the value of $\mu_{n,add}$ is strain independent.

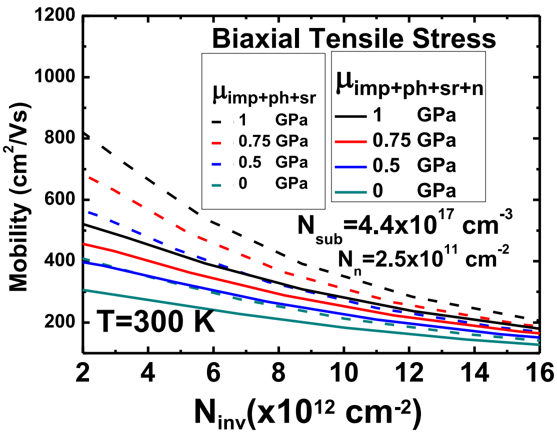

FIGURE 6. **Calculated electron mobility due to the combination of ionized impurity scattering, phonon scattering, and surface roughness scattering, with (solid lines) and without (dashed lines) neutral defect scattering, plotted versus inversion-layer density with biaxial tensile stress as a parameter.**

To make the impact of $\mu_{n,add}$ on the strain altered total effective mobility more visible, here we first define the impact percentage $\gamma (= (\mu_{imp+ph+sr} - \mu_{imp+ph+sr+n})/\mu_{imp+ph+sr+n})$. We transform Fig. 5 and 6 into a single figure: Fig. 7 showing the impact percentage γ for both uniaxial and biaxial stresses. Extra calculation result was also created versus N_n for a fixed N_{inv}, as plotted in Fig. 8. More clearly, the impact of $\mu_{n,add}$ is a strong function of strain, particularly for the weak inversion or high density of neutral defects.

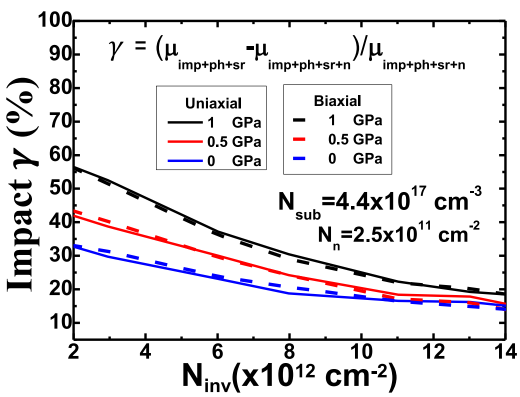

FIGURE 7. **The impact of neutral defect limited mobility on the strain altered total effective mobility according to Fig. 5 and 6.**

IV. EXPERIMENTAL APPLICATION AND VALIDATION

First, we quote the experiment [15] on the strained-silicon SOI MOSFETs undergoing Ge implantation and thermal annealing. The corresponding experimental neutral defect limited mobility $\mu_{n,add}$ of about 1700 cm^2/Vs at N_{inv} of 2×10^{12} cm^{-2} was extracted using Matthiesen's rule (see [15, Figs. 9 and 10]). This corresponds to a neutral defect density N_n of 1.76×10^{11} cm^{-2} according to (10), which is comparable with that ($\sim1.2\times10^{11}$ cm^{-2}) of plan-view TEM images [15], as shown in Fig. 9. The experimentally determined mobility decrease $\eta(\%)$ [15] is plotted in Fig. 10 versus N_{inv}. By definition, $\eta = (\mu_{eff} - \mu_{total})/\mu_{eff}$, where μ_{total} and μ_{eff} are mobility values with and without implantation, respectively. To fit the experimental mobility decrease in Fig. 10, we formulate, from the simulated strain dependent effective mobility μ_{eff} versus N_{inv}, $\mu_{eff} = \beta N_{inv}^{-0.4}$ where β is a constant to be fitted. Then, the total mobility can be obtained using $1/\mu_{total} = 1/\mu_{eff} + 1/\mu_{n,add}$. We find that with $\beta = 6\times10^7$ cm$^{1.2}$/Vs and two N_n values of 1.2×10^{11} and 1.4×10^{11} cm^{-2}, good agreement with data is achieved. Note that the two extracted N_n values are comparable with those of not only the TEM experiment but also the Equation (10).

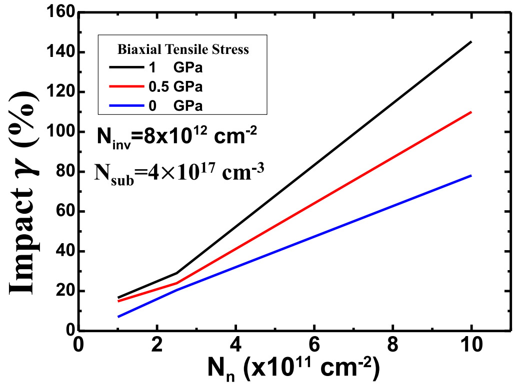

FIGURE 8. **The impact of neutral defect limited mobility on the biaxial strain altered total effective mobility, plotted versus N_n for a fixed N_{inv}.**

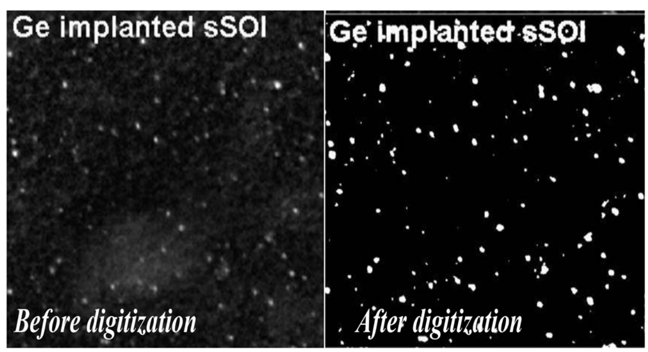

FIGURE 9. **Plan-view TEM images [15] before and after digitization. The neutral defect density is estimated to be around 1.2×10^{11} cm^{-2}. Note that the same digitization technique was also applied in our previous TEM image analysis [6].**

We want to stress that the above formulation $\mu_{eff} = \beta N_{inv}^{-0.4}$ with $\beta = 6\times10^7$ cm$^{1.2}$/Vs can hold for other experiments such as the Si implantation experiment [16]. This is

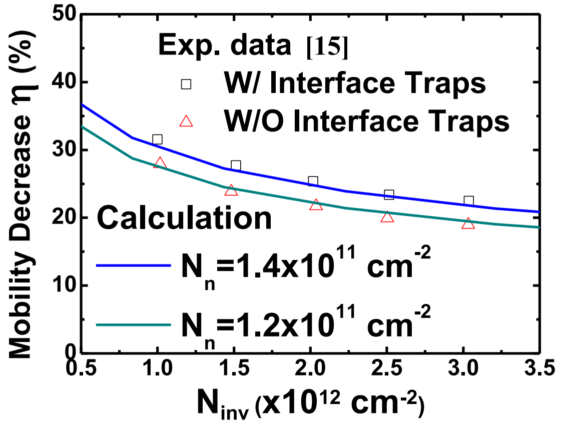

FIGURE 10. **Comparison of experimental (symbols) and calculated (lines) mobility decrease in strained-silicon SOI MOSFETs undergoing Ge implantation and annealing [15].**

the second independent experiment cited in this work. The difference between the Si implantation experiment [16] and the Ge implantation experiment [15] is that only the former can give rise to ionized impurity in strained silicon substrate. Strong evidence can be drawn in Fig. 11. It can be seen that the total silicon electron mobility data [16] can be reproduced in the strong inversion region, except the low N_{inv} region. Such discrepancy dictates the existence of ionized impurity scattering that was absent in the Ge implantation experiment [15].

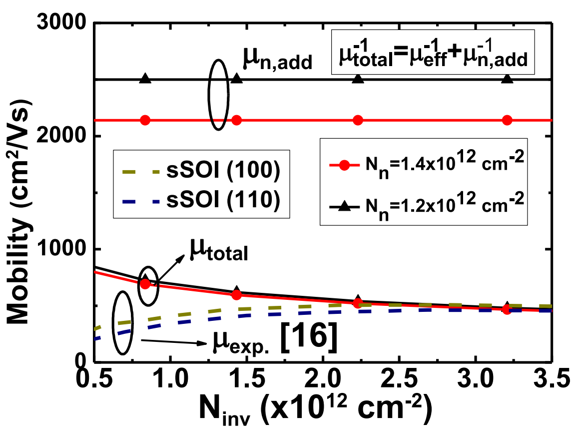

FIGURE 11. **Evidence to support the ability of the formulation of $\mu_{eff} = \beta N_{inv}^{-0.4}$ with $\beta = 6\times10^{7}$ cm$^{1.2}$/Vs to reproduce the independent Si implantation experiment in the strong inversion region [16].**

Finally, we cite the third independent experiment on the Si-implantation-induced performance degradation [17]. In this experiment, the strained Si-based MOSFETs were implanted to examine the damages and their dependence on thermal budgets. Obvious mobility degradation was found even after long annealing time (see [17, Fig. 3(b)]). In this citation [17], no strain relaxation was found and enhanced Ge up-diffusion into the Si layer was determined to be responsible for the mobility degradation.

Using Matthiessen's rule, the corresponding additional scatterers limited mobility due to the implantation can be estimated (see [17, Fig. 3(b)]):

$$\mu_{add}^{-1} = \mu_{implant}^{-1} - \mu_{no\ implant}^{-1} \tag{11}$$

The resulting μ_{add} is plotted in Fig. 12 versus effective electric field E_{eff}, showing a weak dependence on E_{eff} or equivalently N_{inv}. This suggests that the additional scatterers are likely the neutral defects. The corresponding N_n is around 1.8×10^{11} cm^{-2} according to (10). Other scatterers such as alloy scattering [18] and Coulomb-like scattering [19], [20] must be ruled out because they have strong dependencies on N_{inv}.

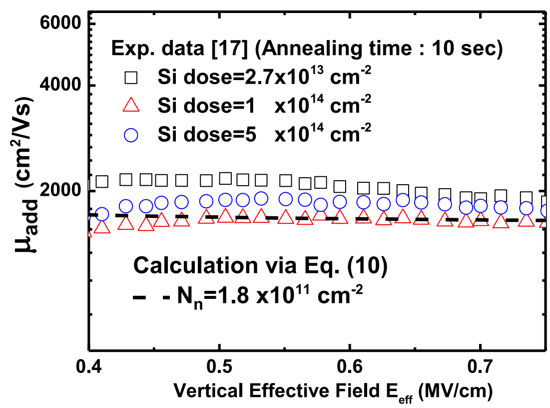

FIGURE 12. **Additional scatterers limited mobility μ_{add} extracted from the experiment [17] and its fitting through Eq. (10) to yield the neutral defect density of around 1.8×10^{11} cm^{-2}.**

Importantly, from the implantation and annealing experiments [15], [17], the two observation points had been drawn that (i) the implantation-induced strain relaxation in strained sample does not occur; and (ii) the neutral defect density is much higher in strained sample than in unstrained sample. Such observations are consistent with our work that strain will not change neutral defect limited mobility unless changing neutral defect density.

V. CONCLUSION

Detailed derivation of the 2D formalism dealing with neutral defect scattering has been presented. New analytical model for neutral defect limited electron inversion-layer mobility has been established. Experimental application and validation of the model have been thoroughly demonstrated. Importantly, this work for the first time corroborates the experimental observations in strained-silicon devices undergoing implantation and annealing.

APPENDIX

First of all, the 3D phase shift in Eq. (1) can be readily applied to 2D case. On the one hand, in the low inversion-layer density region the quantum confinement is weak and the electrons in channel can have 3D-like behavior, thus allowing the use of it. On the other hand, in the high inversion-layer density region the quantum confinement is strong and the average kinetic energy is large. As a consequence, the electrons in the channel are too fast to be captured by the neutral defects, which makes the phase shift $\sin\delta_0 \approx 1$, close to $\sin\delta_0$ of unity in Eq. (1).

Further, we prove that $\sin\delta_0 \approx 1$ is existent in the high inversion-layer density region. By solving two-dimensional Schrödinger equations within and outside of the potential well, one can have two wave functions in a cylindrical coordinate system with ρ as the radial length:

$$\psi_{inside}(\rho) = AJ_0(\alpha_0\rho) \text{ for } 0 < \rho < r_T \tag{A1}$$

and

$$\psi_{outside}(\rho) = B[\cos(\delta_{l=0})J_0(k\rho) - \sin(\delta_{l=0})Y_0(k\rho)] \quad \text{for } r_T < \rho \tag{A2}$$

where $\alpha_0 = \sqrt{\frac{2m^*}{\hbar^2}(\mathrm{E}+\mathrm{V}_0)}$, $k = \sqrt{\frac{2m^*E}{\hbar^2}}$, and J_0 and Y_0 are zero-order Bessel functions. The two constants A and B can be solved by satisfying the following boundary conditions:

$$\psi_{inside}(r_T) = \psi_{outside}(r_T) \tag{A3}$$

$$\frac{d}{d\rho}\psi_{inside}(r_T) = \frac{d}{d\rho}\psi_{outside}(r_T) \tag{A4}$$

Finally, the 2D phase shift is reached for in the functional form:

$$\sin(\delta_0) \approx \sin\left(\tan^{-1}\left\{\frac{kr_TJ_0'(kr_T) - \alpha_0 r_T\frac{J_0'(\alpha_0 r_T)}{J_0(\alpha_0 r_T)}J_0(kr_T)}{kr_TY_0'(kr_T) - \alpha_0 r_T\frac{J_0'(\alpha_0 r_T)}{J_0(\alpha_0 r_T)}Y_0(kr_T)}\right\}\right) \tag{A5}$$

We have calculated that $kr_T \approx \alpha_0 r_T \gg 1$ for large electron energy and thereby this 2D phase shift Eq. (A5) is approximately equal to unity. Therefore, the applicability of Eq. (1) in 2DEG is validated.

REFERENCES

[1] C. Erginsoy, "Neutral impurity scattering in semiconductors," *Phys. Rev.*, vol. 78, pp. 1013–1014, May 1950.
[2] N. Sclar, "Neutral impurity scattering in semiconductors," *Phys. Rev.*, vol. 104, pp. 1559–1561, Dec. 1956.
[3] B. K. Ridley, *Quantum Processes in Semiconductors*. Oxford, U.K.: Clarendon Press, 1988.
[4] K. Seeger, *Semiconductor Physics*, 9th ed. Heidelberg, Germany: Springer-Verlag, 2004.
[5] A. Cros *et al.*, "Unexpected mobility degradation for very short devices: A new challenge for CMOS scaling," in *Proc. IEEE Int. Electron Devices Meeting (IEDM)*, San Francisco, CA, USA, Dec. 2006, pp. 663–666.
[6] S.-H. Hsieh *et al.*, "Two competing limiters in MOSFETs scaling: Neutral defects and S/D plasmons," in *Proc. IEEE Silicon Nanoelectron. Workshop*, Honolulu, HI, USA, Jun. 2016, pp. 32–33.
[7] S. K. Adhikari, "Quantum scattering in two dimensions," *Amer. J. Phys.*, vol. 54, no. 4, pp. 362–367, Apr. 1986.
[8] M. V. Fischetti and S. E. Laux, "Band structure, deformation potentials, and carrier mobility in strained Si, Ge, and SiGe alloys," *J. Appl. Phys.*, vol. 80, no. 4, pp. 2234–2252, Aug. 1996.
[9] D. K. Ferry and S. M. Goodnick, *Transport in Nanostructures*. Cambridge, U.K.: Cambridge Univ. Press, 1999.
[10] M. V. Fischetti, F. Gámis, and W. Hänsch, "On the enhanced electron mobility in strained-silicon inversion layers," *J. Appl. Phys.*, vol. 92, no. 12, pp. 7320–7324, Dec. 2002.
[11] Y. Sun, S. E. Thompson, and T. Nishida, "Physics of strain effects in semiconductors and metal-oxide-semiconductor field-effect transistors," *J. Appl. Phys.*, vol. 101, no. 10, pp. 104503-1–104503-22, May 2007.
[12] M.-J. Chen *et al.*, "Temperature-dependent remote-Coulomb-limited electron mobility in n^+-polysilicon ultrathin gate oxide nMOSFETs," *IEEE Trans. Electron Devices*, vol. 58, no. 4, pp. 1038–1044, Apr. 2011.
[13] M.-J. Chen, C.-C. Lee, and K.-H. Cheng, "Hole effective masses as a booster of self-consistent six-band $k \cdot p$ simulation in inversion layers of pMOSFETs," *IEEE Trans. Electron Devices*, vol. 58, no. 4, pp. 931–937, Apr. 2011.
[14] M.-J. Chen, W.-H. Lee, and Y.-H. Huang, "Error-free Matthiessen's rule in the MOSFET universal mobility region," *IEEE Trans. Electron Devices*, vol. 60, no. 2, pp. 753–758, Feb. 2013.
[15] C. Dupré *et al.*, "Carrier mobility degradation due to high dose implantation in ultrathin unstrained and strained silicon-on-insulator films," *J. Appl. Phys.*, vol. 102, no. 10, pp. 104505-1–104505-8, Nov. 2007.
[16] W. Xiong *et al.*, "Impact of strained-silicon-on-insulator (sSOI) substrate on FinFET mobility," *IEEE Electron Device Lett.*, vol. 27, no. 7, pp. 612–614, Jul. 2006.
[17] G. Xia *et al.*, "Impact of ion implantation damage and thermal budget on mobility enhancement in strained-Si N-channel MOSFETs," *IEEE Trans. Electron Devices*, vol. 51, no. 12, pp. 2136–2144, Dec. 2004.
[18] V. Venkataraman, C. W. Liu, and J. C. Sturm, "Alloy scattering limited transport of two-dimensional carriers in strained Si1-xGex quantum wells," *Appl. Phys. Lett.*, vol. 63, no. 20, pp. 2795–2797, Nov. 1993.
[19] K. Hirakawa and H. Sakaki, "Mobility of the two-dimensional electron gas at selectively doped n-type AlxGa1-xAs/GaAs heterojunctions with controlled electron concentrations," *Phys. Rev. B Condens. Matter*, vol. 33, no. 12, pp. 8291–8303, Jun. 1986.
[20] N. Yang, W. K. Henson, J. R. Hauser, and J. J. Wortman, "Estimation of the effects of remote charge scattering on electron mobility of n-MOSFETs with ultrathin gate oxides," *IEEE Trans. Electron Devices*, vol. 47, no. 2, pp. 440–447, Feb. 2000.

SHANG-HSUN HSIEH received the B.S. degree in physics from National Changhua University of Education, Changhua, Taiwan, in 2010. He is currently pursuing the Ph.D. degree in electronics engineering with the Department of Electronics Engineering and Institute of Electronics, National Chiao Tung University, Hsinchu, Taiwan.

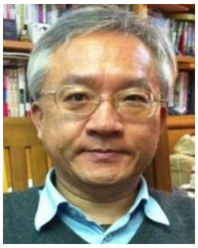

MING-JER CHEN received the Ph.D. degree in electronics engineering from the Department of Electronics Engineering, Institute of Electronics, National Chiao Tung University, Hsinchu, Taiwan, in 1985, where he has been a Professor with the Department of Electronics Engineering, since 1985. He has supervised 22 Ph.D. and over 100 M.S. students, all in the area of device physics.